

Observation of Brillouin scattering from single muscle fibres

N. Berovic¹, N. Thomas¹, R. A. Thornhill², and J. M. Vaughan³

¹ Biophysics Group, School of Physics and Space Research, Birmingham University, Birmingham B15 2TT, UK

² School of Biological Sciences, Birmingham University, Birmingham B15 2TT, UK

³ Royal Signals and Radar Establishment, St. Andrews Road, Great Malvern, Worcester, UK

Received November 3, 1988/Accepted in revised form March 10, 1989

Abstract. The propagation of sound waves along relaxed single fibres of glycerinated rabbit psoas muscle has been observed using Brillouin scattering at frequencies up to 1.6 GHz. Two types of waves were observed: one with a velocity of $1508 \pm 7 \text{ m s}^{-1}$, which is attributed to sound waves in intra-cellular saline, the other with a velocity of $912 \pm 25 \text{ m s}^{-1}$, which is attributed to waves propagating along the protein filaments within individual sarcomeres. The latter sound velocity is much higher than that which has been reported by Stienen and Blangé (1985) for 50 μs tension transients, and the difference is attributed to the much higher stiffness of the protein filaments compared to the cross-bridges which determine the low-frequency elasticity of muscle fibres.

Key words: Muscle, sound velocity, Brillouin scattering

Introduction

From a physical point of view, the propagation of sound waves along the one-dimensional periodic array of sarcomeres in muscle myofibrils represents an interesting problem. However, very little is in fact known about the elastic properties of muscle at frequencies above those which are of direct interest in muscle physiology, where measurements are usually performed below 1 kHz. We have undertaken to investigate sound-wave propagation at very high frequencies along glycerinated single muscle fibres by means of Brillouin light scattering, since this technique allows us to study sound waves with a wavelength comparable to the sarcomere size. We believe that this is the first time that Brillouin scattering has been observed from viable muscle fibres, although measurements on dried muscle were reported by Harley et al. (1977) some years ago.

Brillouin scattering is the scattering of light by thermally generated sound waves inside a material. It

is a well established technique in condensed-matter physics (Dil 1982), and in biophysics the technique has been used to study collagen (Harley et al. 1977; Cusack and Miller 1979), the eye lens and cornea (Vaughan and Randall 1980; Randall and Vaughan 1982), and also DNA (Maret et al. 1979; Hakim et al. 1984). Although the detailed theory of Brillouin scattering is beyond the scope of this paper (see, for instance, Dil 1982 or Fabelinskii 1968), the basic principles can be understood with reference to the vector triangle shown in the inset to Fig. 1. Here, incident light of wavevector \mathbf{k}_0 is scattered through an angle θ by a sound wave of wavevector \mathbf{q} inside the sample. The scattered light undergoes a very small frequency shift, equal to the sound-wave frequency. Hence the incident and scattered wavevectors, \mathbf{k}_0 and \mathbf{k}_1 , have almost exactly the same magnitude, and it follows from the isosceles vector triangle that the magnitude of the scattering wavevector \mathbf{q} is

$$q = \frac{4\pi}{\lambda} \sin \frac{\theta}{2}, \quad (1)$$

where λ is the wavelength of the incident light. The frequency ν of the sound wave is thus given by

$$\nu = \frac{2v}{\lambda} \sin \frac{\theta}{2}, \quad (2)$$

where v is the velocity of sound. Equation (2) therefore determines the frequency shift for Brillouin scattering of light through an angle θ , and the measurement of this frequency shift allows the velocity of sound to be determined.

In practice, the spectrum of the scattered light consists of an unshifted *Rayleigh* component together with Brillouin components at both lower and higher frequency (sometimes called the Stokes and anti-Stokes lines), whose frequency shift is determined by Eq. (2). Rayleigh scattering from muscle is particularly strong because muscle fibres produce a distinctive optical diffraction pattern (Rüdel and Zite-Ferenczy

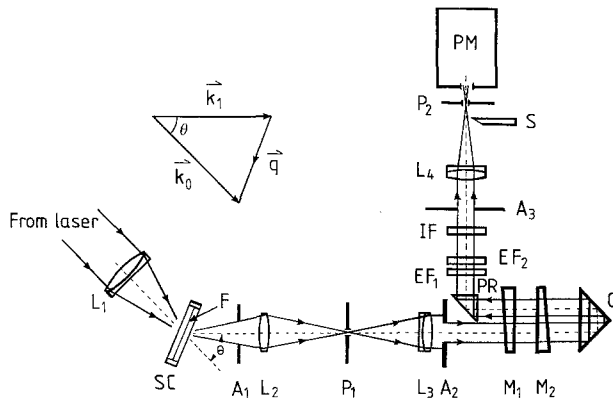


Fig. 1. Simplified diagram of the optical apparatus as described in the text. Note that the interferometer is drawn as two-pass rather than four-pass for clarity. A_1 – A_3 – apertures; C – corner-cube; EF_1 and EF_2 – edge filters; F – muscle fibre; IF – interference filter; L_1 – L_4 – lenses; M_1 and M_2 – interferometer mirrors; P_1 and P_2 – pinholes; PM – photomultiplier; PR – prism; S – shutter; SC – sample cell. The inset shows the vector triangle appropriate to Brillouin scattering of a light wave of incident wavevector \mathbf{k}_0 into a scattered wave \mathbf{k}_1 by a sound wave of wavevector \mathbf{q} .

1979; Baskin et al. 1981). Hence the observation of Brillouin scattering from muscle requires special precautions, which are discussed in detail in the following section.

Since Brillouin scattering is produced by thermally generated sound waves inside the muscle, it is not necessary to attach a conventional ultrasonic transducer to the sample. This would in any case be impracticable for a single muscle fibre at the frequencies of 1 GHz or more which are accessible using the Brillouin technique. Conventional ultrasonics techniques are limited to much lower frequencies; for instance, Hatta et al. (1984) have used conventional ultrasonics to study bulk muscle at frequencies up to 7 MHz. At still lower frequencies, Stienen and Blangé (1985) used a very fast mechanical servo system to study the propagation of tension transients (rise time $\sim 50 \mu\text{s}$) in single muscle fibres. In both of these experiments the sound wavelength was much greater than the sarcomere repeat distance, whilst in our Brillouin measurements the wavelength is in fact somewhat smaller than the sarcomeres themselves. We have therefore been able to measure the elastic properties of muscle in a regime which has not previously been investigated.

Materials and methods

Fibre preparation

All of the muscle fibres used in this investigation were dissected from glycerinated rabbit psoas muscle. Small

bundles (0.5–1 mm in diameter) of muscle fibres were prepared following the procedure of Brenner (1983) and were stored in 50% glycerol at -20°C for up to four weeks. Single fibres were dissected out in relaxing solution containing 5 mM ATP (Brenner 1983) and were mounted in this solution inside a stainless-steel sample cell of dimensions $16 \times 4 \times 4$ mm, whose front and rear faces were made from microscope coverslips to serve as optical windows. Fibres were glued with cellulose acetate to stainless-steel pins protruding through narrow slots in the ends of the cell. Care was taken during dissection and mounting to ensure that the fibres were not twisted. The fibre length was adjusted by micrometer movements attached to the pins, and all measurements were performed with fibres in the relaxed state at a sarcomere length of $3 \mu\text{m}$, as determined from the optical diffraction pattern. This length was chosen to allow Brillouin measurements to be performed between diffraction orders as described below.

Optical apparatus and procedure

From an experimental point of view, the detection of Brillouin scattering from muscle fibres with a frequency shift of 1 GHz or less requires an optical system of very high performance. In the first place, since the frequency shift is only about one millionth of the light frequency itself, a spectrometer of high resolution is required. This may be achieved using a Fabry-Pérot interferometer, which basically consists of two parallel plane mirrors of variable separation. The interferometer behaves as a narrow-band optical filter whose transmission peak is scanned across the optical spectrum by varying the mirror separation. Peak transmission is in fact a resonance phenomenon, occurring whenever the mirror separation d is an integral number of half wavelengths, which means that transmission peaks occur for optical frequencies at intervals of $c/2d$, where c is the speed of light. The spacing of transmission peaks is known as the free spectral range, and for a mirror separation of 7.5 cm this is 2 GHz, effectively defining the frequency range of the spectrometer. The frequency resolution of the interferometer is limited by the sharpness of the transmission peaks, which is determined by the reflectivity of the mirrors: it is customary to characterize this by the “finesse” of the interferometer, which is the ratio of its free spectral range to the width of the transmission peaks. A finesse of 40 is typical, implying a frequency resolution of about 50 MHz at a free spectral range of 2 GHz.

A further consideration in the optical design is the need to separate the weak Brillouin components in the scattered light from the unshifted Rayleigh compo-

nent. Muscle fibres produce striking optical diffraction patterns, and there is also a certain amount of diffuse scattering between diffraction orders. Hence Rayleigh scattering by muscle is very strong indeed, and this elastically scattered light enters the interferometer along with the frequency shifted, but much less intense, Brillouin components. The ability of the interferometer to reject unwanted light of a different frequency is measured by its contrast ratio, which is the ratio of maximum and minimum transmission coefficients, minimum transmission occurring at the centre of a free spectral range. The contrast ratio of a Fabry-Pérot interferometer may be greatly enhanced by means of multi-pass operation (Sandercock 1975), in which corner-cube prisms are used as retro-reflectors to pass the light beam through the same interferometer several times. With such an arrangement, Brillouin scattering may be detected using a photomultiplier at the output of the interferometer even in the presence of quite intense Rayleigh scattering.

A simplified diagram of the optical apparatus which we have used is shown in Fig. 1. Highly monochromatic light of wavelength 488 nm was produced by a single-mode argon-ion laser (Spectra-Physics Model 171 with intra-cavity etalon), and the light scattered by a muscle fibre was analysed using a piezoelectrically scanned four-pass Fabry-Pérot interferometer (drawn as two-pass for simplicity). The interferometer was fitted with dielectric-coated mirrors (IC Optical Systems, Beckenham, Kent UK), which were optically flat to $\lambda/150$ with a reflectivity of 94% and absorption of $<0.5\%$. Very precise collimation was provided by 50 μm diameter entrance and exit pinholes together with 160 mm focal-length achromatic aplanatic collimator lenses working at an aperture of $f/50 - f/30$.

The resulting instrumental finesse at a free spectral range of 2.04 ± 0.02 GHz was about 40, and we achieved a measured contrast ratio of 10^9 with a peak transmission efficiency of 2%. An image-quality interference filter (bandwidth 1 nm, transmission 55%) was used to block fluorescence from the muscle, and additional broadband filters and a dispersing prism (not shown) were used to reject fluorescence from the laser gas discharge. The overall efficiency of the interferometer together with the optics and the photon-counting system (dark count-rate 10 s^{-1}) for light entering the front pinhole was typically 0.03%.

In operation, 100 mW of laser light was focussed onto the muscle fibre by an 80-mm focal-length achromat to produce a diffraction-limited "streak" at the focus of width $\sim 50 \mu\text{m}$, which was imaged onto the front pinhole by a 75-mm focal-length microscope objective operating at unity magnification. The focussed beam and imaging optics ensured efficient collection of the scattered light, and the narrow streak minimized refraction by the cylindrical fibre. Prolonged exposure

of the fibre to the focussed beam was avoided, data accumulation typically requiring about two minutes using a Z80-based microcomputer. An electronically triggered shutter was used to protect the photomultiplier each time the interferometer scanned through the intense Rayleigh peak from muscle, and the trigger signal was also used to lock the interferometer scan to the laser frequency, thus compensating for small frequency drifts in the system. Single-mode operation of the laser was ascertained independently during data accumulation using a photodiode and a spectrum analyser capable of detecting inter-mode beats. This system was also used in a separate experiment to calibrate the free spectral range of the interferometer by deliberately tilting the laser's intra-cavity etalon until additional laser modes appeared.

The precise scattering geometry shown in Fig. 1 is rather important and was chosen to look for Brillouin scattering from sound waves propagating *along* a muscle fibre. The muscle fibre was mounted parallel to the refracting faces of the sample cell, which was oriented so that the fibre bisected the angle between the incident and scattered light beams. This ensured that the scattering wavevector was parallel to both the fibre axis and the refracting interfaces in the cell. Now, when light is refracted at an interface the component of its wavevector *parallel* to the interface is unchanged owing to the requirement of matching wavefronts across the interface. Hence the scattering wavevector in our arrangement is unaffected by refraction. The Brillouin shift is therefore given by Eq. (1), in which, by virtue of the special geometry, the laser wavelength λ and the scattering angle θ may be measured in air *outside* the scattering cell.

Results

An example of the Fabry-Pérot spectrum for light scattered from saline solution at an angle of 21.2° is shown in Fig. 2a. The peaks labelled R_1 and R_2 are both due to the unshifted Rayleigh component, which produces a peak each time the resonance condition is satisfied for light at the laser frequency. The separation of the Rayleigh peaks therefore corresponds to a single free spectral range of the interferometer. The peaks labelled S_1 and S_2 are due to Brillouin scattering from sound waves in the saline. The frequency shift in this case is 1.13 GHz, so that in fact Brillouin peak S_1 is associated with Rayleigh peak R_1 , and S_2 is associated with R_2 .

Figure 2b shows the spectrum for light scattered from a single muscle fibre in the same saline solution and at the same scattering angle of 21.2° . These results were obtained shortly after those shown in Fig. 2a by slightly displacing the sample cell vertically to bring

Table 1. Brillouin frequencies S_1 , S_2 , M_1 and M_2 obtained from muscle spectra similar to Fig. 2b at different scattering angles θ for a total of six fibres. The average frequencies \bar{S} and \bar{M} for the saline and muscle peaks at each angle are also shown along with the corresponding sound velocities v_s and v_m calculated using Eq. (2)

Fibre	θ	S_1 [GHz]	S_2 [GHz]	\bar{S} [GHz]	v_s [m s ⁻¹]	M_1 [GHz]	M_2 [GHz]	\bar{M} [GHz]	v_m [m s ⁻¹]
1	21.2°	1.132	1.132	1.132	1,500	0.710	0.655	0.669	886
		—	—			0.655	0.655		
2	22°	1.188	1.166	1.174	1,502	0.710	0.688	0.694	887
		1.166	1.177			—	—		
3		—	—			0.677	0.699		
4	30°	1.587	1.632			1.032	1.032		
5		1.643	1.610			1.055	1.055		
6		1.665	1.554	1.615	1,523	0.999	0.999	1.021	963
		—	—			0.999	0.999		

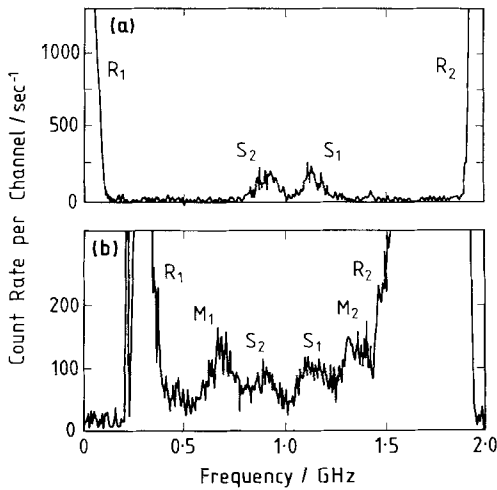


Fig. 2a and b. Fabry-Pérot spectra for light scattering from (a) saline and (b) a relaxed glycerinated rabbit psoas muscle fibre, both at a scattering angle of 21°. Peaks labelled R_1 and R_2 are due to Rayleigh scattering. Brillouin peaks from saline S_1 and S_2 with a frequency shift of 1.13 GHz are present in both (a) and (b). Additional Brillouin peaks M_1 and M_2 with a frequency shift of 669 MHz present are in the spectrum from muscle and are attributed to sound waves propagating along the muscle fibre. Note that the intense Rayleigh scattering from muscle was partly blocked by a shutter and that different vertical scales are used in (a) and (b). The channel width for both measurements was 6.18 MHz

the muscle fibre into the focussed laser beam. Brillouin peaks at the same frequency as for saline, again labelled S_1 and S_2 , are present in the spectrum from muscle. In addition, there are new Brillouin peaks, labelled M_1 and M_2 , which are characteristic of muscle itself. Brillouin peaks were only observed for fibres with well defined diffraction patterns, indicative of an ordered sarcomere lattice. The experiment was repeated at a scattering angle of 30°, in which case the two Brillouin peaks from muscle were superimposed at the centre of the free spectral range. A Brillouin shift of 1.02 GHz at this angle was established by repeating

the measurement with a free spectral range of 2.25 GHz to separate the peaks. The measurement at 21.2° was also repeated with the new free spectral range to check for the possibility of overlapping of orders in the Fabry-Pérot spectrum. This allowed us to assign a definite Brillouin shift of 669 ± 14 MHz to the muscle peaks in Fig. 2b. A complete tabulation of all our Brillouin measurements to date on a total of six fibres is presented in Table 1, and these results are discussed in detail in the following section.

The Rayleigh peaks R_1 and R_2 shown in Fig. 2b for muscle are far more intense than those for saline in Fig. 2a. We were obliged to work between diffraction orders, so that the interferometer only had to cope with the less intense diffuse Rayleigh scattering, which was typically about 1 μ W at the input to the interferometer. The most intense parts of the Rayleigh peaks in Fig. 2b were blocked by the shutter and would correspond to $\sim 10^7$ times the intensity of the Brillouin peaks. The shutter trigger signal was used to lock the interferometer scan to the laser, so frequency drift in the laser is not therefore responsible for the broadening of the Brillouin peaks in muscle. If this broadening were solely due to attenuation of the sound waves then it would imply an attenuation distance of only a few wavelengths. This illustrates how difficult it would be to study sound waves in muscle at 1 GHz using conventional ultrasonics techniques.

Discussion

Our results in Fig. 2b demonstrate the feasibility of observing Brillouin scattering from single muscle fibres under physiological conditions. Two distinct Brillouin signals are observed: first the peaks S_1 and S_2 , which occur at the same frequency as for Brillouin scattering in saline, and second the peaks M_1 and M_2 which have a smaller Brillouin shift and which are only

observed in well-ordered muscle fibres exhibiting a distinct diffraction pattern.

The frequencies of the Brillouin peaks S_1 and S_2 in muscle are tabulated in Table 1 for scattering angles of 21.2° , 22° and 30° . The average frequency shift \bar{S} is also shown for each angle, and in each case the frequency shift determined from the Brillouin spectrum for muscle agreed with that measured separately in saline. The sound velocity in saline v_s has been calculated for each angle using Eq. (2), and the values obtained at the three angles are equal to within 1.5%. As one would expect, this implies that there is no significant dispersion for the sound velocity in saline in the frequency range 1.1–1.6 GHz covered by these measurements. The average sound velocity for the three angles is $1508 \pm 7 \text{ m s}^{-1}$, in very good agreement with the velocity of $1505 \pm 30 \text{ m s}^{-1}$ which we measured separately using conventional ultrasonics in saline at 5 MHz.

The frequencies of the Brillouin peaks M_1 and M_2 in muscle are also tabulated in Table 1 along with the average frequency \bar{M} and the corresponding sound velocity v_m for each scattering angle. The sound velocities at 21.2° and 22° are found to be 886 m s^{-1} and 887 m s^{-1} respectively, but at 30° we find a sound velocity of 963 m s^{-1} . Although this might represent genuine dispersion inside the muscle fibre, we feel that at present this conclusion would be premature. This is because we sometimes observed for Brillouin spectra at 22° that the saline and muscle peaks overlapped. This would imply a higher average frequency \bar{M} at 22° than is suggested by the results in Table 1, which are necessarily based on spectra where the Brillouin peaks were resolved from each other. We have therefore taken the representative velocity for the sound waves producing peaks M_1 and M_2 in muscle to be the average value of $912 \pm 25 \text{ m s}^{-1}$.

The velocity $912 \pm 25 \text{ m s}^{-1}$ which we have obtained for sound propagation along muscle fibres is considerably higher than the velocity of $112 \pm 6 \text{ m s}^{-1}$ obtained by Stienen and Blangé (1985) for tension transients in relaxed frog ileofibularis muscle fibres. In their low-frequency experiment the sound wavelength is very long ($\sim 5 \text{ cm}$ at 20 kHz), so the sound velocity reflects the elastic behaviour of entire myofibrils containing many sarcomeres. It is therefore presumably the elasticity of the cross-bridges linking the protein filaments which is crucial in determining the velocity of the tension transients, and this view is supported by the increase in the sound velocity to $230 \pm 10 \text{ m s}^{-1}$ which Stienen and Blangé observed in active muscle. In contrast, the wavelength of the sound waves in our experiment is only $\sim 1 \mu\text{m}$, which is in fact somewhat smaller than the sarcomere repeat distance of $3 \mu\text{m}$. At such short wavelengths there must be distortion of the protein filaments themselves, rather than just a change

in filament overlap, and this will lead to a higher sound velocity, characteristic of waves within single sarcomeres. The high velocity which we have measured in relaxed muscle may therefore be due to the much higher stiffness of the protein filaments compared to the cross-bridges. In suggesting this interpretation we are implicitly assuming that our Brillouin peaks are due to *longitudinal*, rather than *transverse*, waves and we intend to test this hypothesis in due course.

It is also possible to reconcile our results with those of Hatta et al. (1984), who found a velocity of $1600 \pm 50 \text{ m s}^{-1}$ for longitudinal waves in bulk muscle at 7 MHz. Their velocity is close to the velocity of $1508 \pm 7 \text{ m s}^{-1}$ for the saline peaks S_1 and S_2 in Fig. 2b, which we believe to be due to sound waves propagating in *intra-cellular* fluid inside the muscle fibre. Our imaging arrangement shown in Fig. 1 rejects almost all of the light scattered from saline outside the fibre, but it is clear from Fig. 2 that the integrated intensity under the saline peaks in muscle is comparable to that in pure saline. We therefore believe that the saline peaks in muscle originate from the intra-cellular fluid which accounts for $\sim 80\%$ of the volume of muscle. This may also be the medium for the sound-wave propagation studied by Hatta et al., since it is quite possible that waves propagating along the sarcomere lattice itself at 7 MHz are too strongly attenuated by relaxation processes to be detected using conventional ultrasonics with a transducer spacing of 2 cm. In that case, only the signal propagating in the intra-cellular fluid would be detected. We note that Hatta et al. in fact saw only a small change in sound velocity (about 10 m s^{-1}) compared to that seen by Stienen and Blangé (1985) when the muscle was active.

In conclusion, we have shown that Brillouin scattering can be used to study the propagation of gigahertz sound waves in single muscle fibres under physiological conditions. We hope in the future to investigate the effects of changing the physiological state of the fibres and of varying the sarcomere repeat distance. It would also be of interest to extend these measurements to other types of muscle and, if possible, to perform measurements at somewhat lower frequencies so that the sound wavelength becomes comparable to or greater than the sarcomere repeat distance.

Acknowledgements. We gratefully acknowledge invaluable technical assistance from Mr. J. Harling, support from Profs. P. J. Butler, D. C. Colley and W. F. Vinen, and much encouragement from Prof. G. R. Isaak.

References

- Baskin RJ, Lieber RL, Oba T, Yeh Y (1981) Intensity of light diffraction from striated muscle as a function of incident angle. *Biophys J* 36:759–773

- Brenner B (1983) Technique for stabilizing the striation pattern in maximally calcium-activated skinned rabbit psoas fibres. *Biophys J* 41:99–102
- Cusack S, Miller A (1979) Determination of the elastic constants of collagen by Brillouin light scattering. *J Mol Biol* 135:39–51
- Dil JG (1982) Brillouin scattering in condensed matter. *Rep Prog Phys* 45:285–334
- Fabelinskii IM (1968) *Molecular scattering of light*. Plenum Press, New York
- Hakim HB, Lindsay SM, Powell J (1984) The speed of sound in DNA. *Biopolymers* 22:1185–1192
- Harley R, James D, Miller A, White JW (1977) Phonons and the elastic moduli of collagen and muscle. *Nature* 267:285–287
- Hatta I, Tamura Y, Matsuda T, Sugi H, Tsuchiya T (1984) Muscle stiffness changes during isometric contraction in frog skeletal muscle as studied by the use of ultrasonic waves. *Adv Exp Med Biol* 170:673–684
- Maret G, Oldenbourg R, Winterling G, Dransfeld K, Rupprecht A (1979) Velocity of high frequency sound waves in oriented DNA fiber and films determined by Brillouin scattering. *Colloid Polym Sci* 257:1017–1020
- Randall J, Vaughan JM (1982) The measurement and interpretation of Brillouin scattering in the lens of the eye. *Proc R Soc Lond B* 214:449–470
- Rüdel R, Zite-Ferenczy F (1979) Interpretation of light diffraction by cross-striated muscle as Bragg reflection by the lattice of contractile proteins. *J Physiol (London)* 290:317–330
- Sandercock JR (1975) Some recent developments in Brillouin scattering. *RCA Rev* 36:89–107
- Stienen GJM, Blangé T (1985) Tension responses to rapid length changes in skinned muscle fibres of the frog. *Pflügers Arch* 405:5–11
- Vaughan JM, Randall J (1980) Brillouin scattering, density and elastic properties of the lens and cornea of the eye. *Nature* 284:489–491